machines

Article

Analysis of the Design of the Single-Cylinder Steam Engine of the Grasshopper Beam by Henry Muncaster

José Ignacio Rojas-Sola [1,*] and José Francisco Gutiérrez-Antúnez [2]

[1] Department of Engineering Graphics, Design and Projects, University of Jaen, 23071 Jaen, Spain
[2] Higher Polytechnic School, University of Jaen, 23071 Jaen, Spain
* Correspondence: jirojas@ujaen.es; Tel.: +34-953-212452

Abstract: In this paper, the analysis of the design of the single-cylinder steam engine of the Grasshopper beam designed by Henry Muncaster in 1912 is shown. This engine was incorporated into ships and railways and it was published in the *Model Engineer* journal in 1957. It shows great complexity due to its ability to transform reciprocating movement into rotary movement and its high number of elements (more than 150). To this end, a study of computer-aided engineering (CAE) was carried out using the software Autodesk Inventor Nastran, consisting of a linear static analysis using the finite element method (FEM) of the 3D CAD model under real operating conditions in order to learn if it was well designed, according to material resistance criteria. The assembly is analyzed in the two most unfavorable situations in order to determine the von Mises stresses, the displacements and the safety coefficient distributions. Finally, it was found that the work pressure (maximum admissible steam pressure in the admission) was 0.15 MPa.

Keywords: Henry Muncaster; steam engine; grasshopper beam; Autodesk Inventor Nastran; computer-aided engineering; finite-element analysis

check for updates

Citation: Rojas-Sola, J.I.; Gutiérrez-Antúnez, J.F. Analysis of the Design of the Single-Cylinder Steam Engine of the Grasshopper Beam by Henry Muncaster. *Machines* **2023**, *11*, 703. https://doi.org/10.3390/machines11070703

Academic Editors: Martin Pollák and Marek Kočiško

Received: 11 June 2023
Revised: 27 June 2023
Accepted: 28 June 2023
Published: 2 July 2023

1. Introduction

Steam engines have historically been one of the most widely used inventions in engineering, mainly between the 18th and 19th centuries when steam was the most commonly used form of energy. In reality, they are constituted as thermal machines, where the expansion of the steam occurs, transforming the heat energy into mechanical energy (work), whose magnitude will depend on the temperature gradient between the temperature of the steam at the entrance and the temperature of steam at the outlet of the machine [1,2].

Among the first to put this machine into service were Papin, Savory and Newcomen; Humphrey Potter, who originated the automatic operation of the valves; James Watt [3], who invented the separate condenser; and Trevithick, Hedley and Hackworth, the pioneers of the locomotive. Thus, it is a machine that has been used for different purposes and implemented in different means of locomotion, such as ships or railways, and that has undergone modifications to improve its efficiency and economy.

Henry Muncaster was an English engineer who was born in the second half of the 19th century, an expert in everything related to steam engines and who developed his work in the mining, coal, steel and large pumping industries [4]. From the beginning of the 20th century, he contributed numerous articles to the *Model Engineer* magazine until his death in 1935, and in 1912, he published a book presenting eight stationary steam-powered devices [5]. The present investigation analyses one of his inventions, the Grasshopper beam steam engine, from an engineering viewpoint [6,7].

Recently, an investigation carried out by the authors allowed us to obtain the 3D CAD model of this invention [8] from the plans of Julius de Waal [7], in which the operation of the device is explained in detail and on which this analysis is based.

The grasshopper beam steam engine pivots at one end rather than the center, and usually, the connecting rod of the crankshaft is positioned between the piston and the pivot, i.e., they act as a lever of the second kind [9]. In this way, a long stroke is produced for the piston with a shorter stroke for the crank, albeit with greater force.

The first recorded example was William Murdoch's model steam carriage of 1784 [10], although later its use was extended mainly to marine engines. Unlike conventional beam engines that required masonry construction to house the heavy beam and pivot, the grasshopper beam was pivoted on a swinging link. Thus, they were much lighter and their use spread to smaller engines [6]. Furthermore, although the weight of the Grasshopper beam is completely unbalanced, the fact that it is much lighter than the conventional beam allows Grasshopper engines to perform satisfactorily at higher speeds than conventional beam engines [7].

Moreover, there is no worldwide study of this engine from the point of view of engineering, which underlines the novelty, originality and scientific interest of this work. For this reason, the ultimate goal of this study was to perform a static analysis [11] of the single-cylinder steam engine of the grasshopper beam using the finite element method [12] under real operating conditions in order to determine whether it was properly designed and show how the model could be optimized by determining the work pressure (maximum admissible steam pressure in the admission).

The remainder of the paper is structured as follows: Section 2 shows the materials and methods (including the machine's operation) used in this research, Section 3 includes the main results (modal analysis and static analysis) and discussion, and Section 4 presents the main conclusions.

2. Materials and Methods

The starting material for this research was based on the 3D CAD model, obtained previously [8] using the Autodesk Inventor Professional software [13], to carry out a computer-aided engineering study, particularly a linear static analysis, using Autodesk Inventor Nastran [14]. This is a powerful software for the numerical simulation of engineering problems; particularly, it is a calculation engine for the finite element method that is well recognized in mechanics.

This section briefly explains the operation of the steam engine under study, in order to provide a better conceptualization of the analysis carried out and the working hypotheses from the design point of view, detailing each of the previous phases before executing linear static analysis. In this analysis, two of the most notable variables are the von Mises stress and the displacements suffered by the components of the machine, since these variables mechanically characterize the behavior of the assembly, verifying that its operation under real operating conditions is completely safe.

2.1. Operation of the Machine

Although the detailed operation of the machine is explained in detail in a recent investigation carried out by the authors [8], where detailed information on the modeling and assembly process can be obtained (Figure 1), a brief summary is presented below.

This machine is made up of a single double-acting cylinder. Therefore, the working fluid (water vapor) enters and leaves on both sides of the piston, thus carrying out two thermodynamic cycles simultaneously (although out of phase; for example, while on one side of the piston, the admission of water vapor occurs, on the other, the escape occurs). Intake and exhaust control are carried out through a slide valve inside the slide valve chest block, which is located next to the piston cylinder. The movement of this slide valve is due to a linkage, whose relative movement between parts is produced thanks to the coupling of the connecting rod of the slide valve to the crankshaft. An eccentric sheave is attached to it in order to synchronize the movement of the piston with the movement of the slide valve so that the admission and exhaust of the steam are carried out during certain periods of time, thus achieving good operation of the machine.

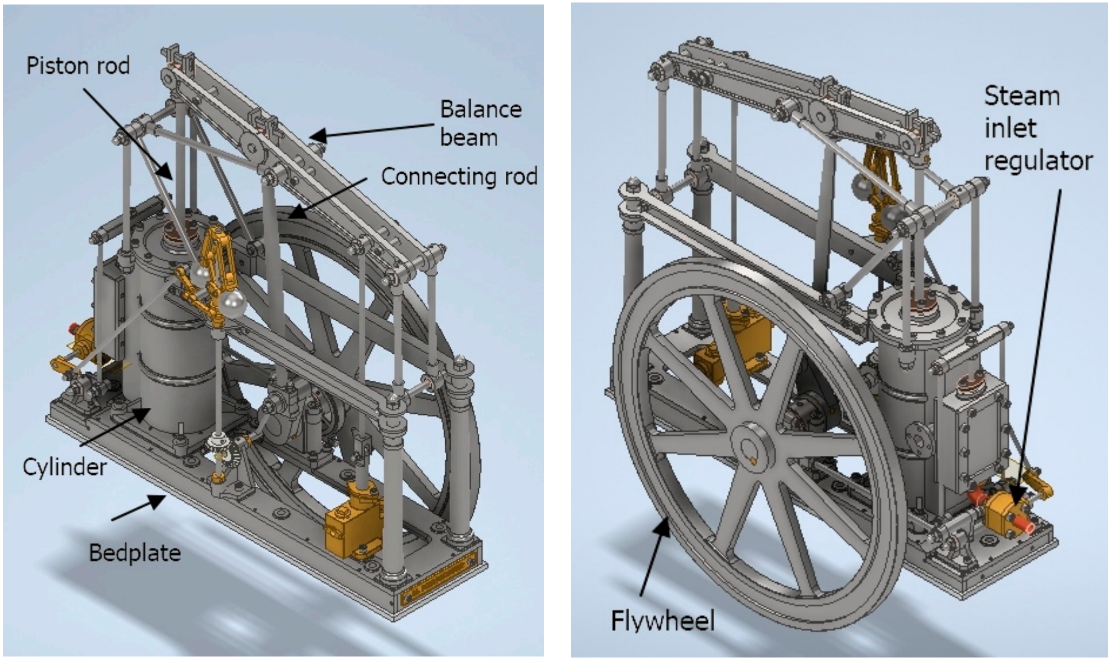

Figure 1. Assembly of the machine: front view (**left**) and rear view (**right**).

A notable element of the machine and its design is the master linkage used to transform the reciprocating movement of the piston into a rotary movement of the crankshaft (Figure 2). For this, a balance beam is used, located in the upper part of the invention, which allows a lightening of the weight of the machine.

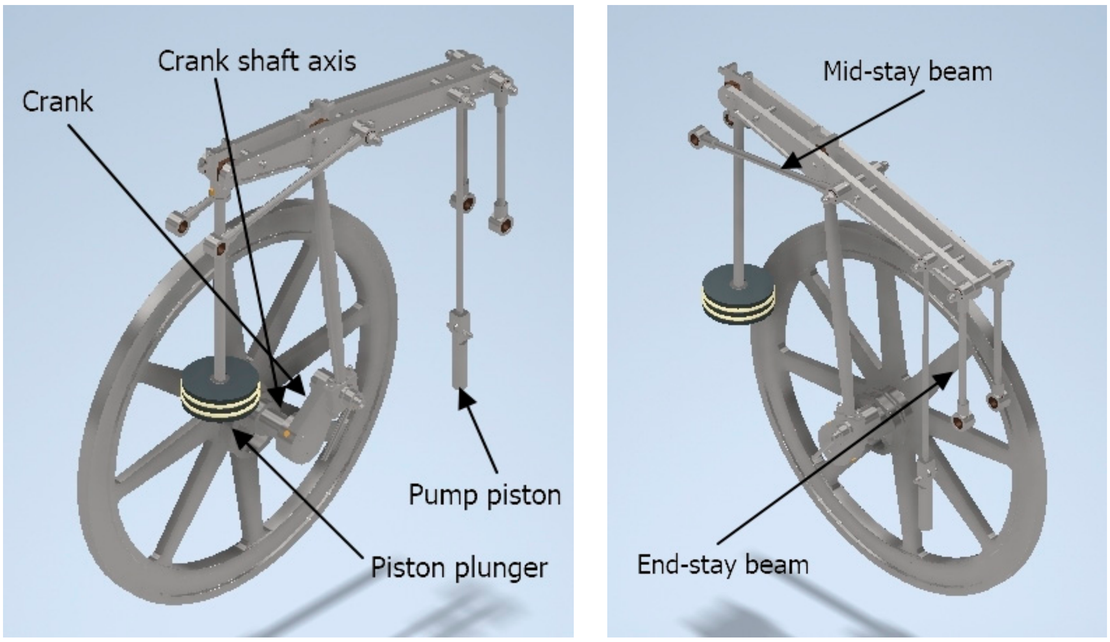

Figure 2. Master linkage: front view (**left**) and rear view (**right**).

In addition, a connecting rod with a piston at its end is attached to the balance beam, which will have an alternative movement inside a pump to compress the water vapor and propel it from the tank to the boiler, from where it will come out with higher pressure and temperature, to later expand in the cylinder chamber and transform the thermal energy into mechanical energy, which will be used thanks to the flywheel.

A great advantage of this machine, in addition to the one mentioned above, is its ability to self-regulate and keep working under stationary conditions. For this, a speed regulator is used (Figure 3) with a very specific function: to regulate the flow of steam inlet to the slide valve chest block by turning a valve that will increase or decrease the cross-section inside the steam inlet housing. As a consequence, if the velocity of the fluid through the cross-section changes, the flow will also change. In this invention, the rotation of this valve is carried out automatically, being controlled by the speed regulator.

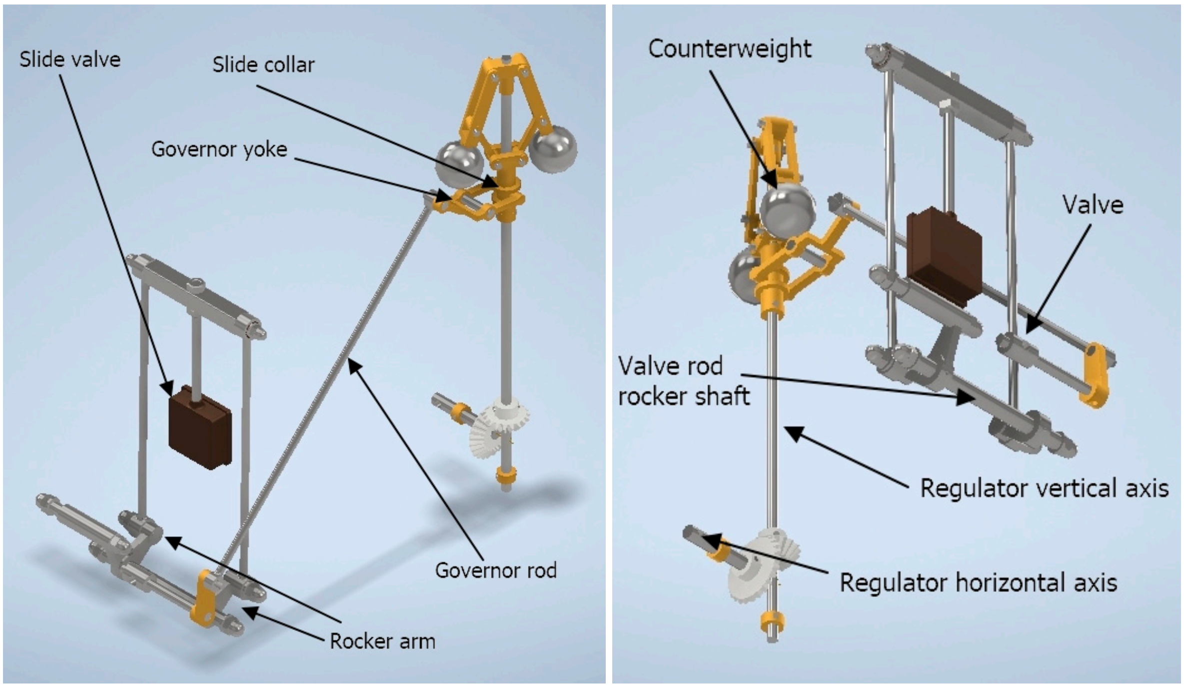

Figure 3. Speed regulator: top view (**left**) and bottom view (**right**).

To accomplish this, the speed regulator is made up of two axes, one horizontal and the other vertical, each with its respective components. The horizontal axle is coupled to the crankshaft, and at its end is a gear that transmits the rotational movement from the horizontal axle to the vertical axle. At the opposite end of the vertical axle gear, there is a small linkage, formed by two articulated quadrilaterals, with some counterweights at the end of one of its links. Since the shaft rotates, these counterweights produce a centrifugal force that depends on the speed of rotation of the shaft and its angular acceleration. This causes the sliding collar of the speed regulator to move vertically, moving a yoke which in turn is connected to a bar that will rotate the valve connecting rod, producing its rotation and varying the inlet flow. Therefore, depending on the speed of the crankshaft, the centrifugal force exerted will vary and, consequently, the position of the sliding collar, thus regulating the inlet flow of water vapor. In this way, the speed of rotation of the flywheel is always the same and the steam engine works under stationary conditions since these steam engines were installed in trains or boats, with the speed constant through almost the entire displacement.

Figure 4 shows an axonometric view and a front view of the sectioned invention, in order to more clearly observe the elements that make up the machine, as well as the interior of the cylinder chamber and the slide valve chest block.

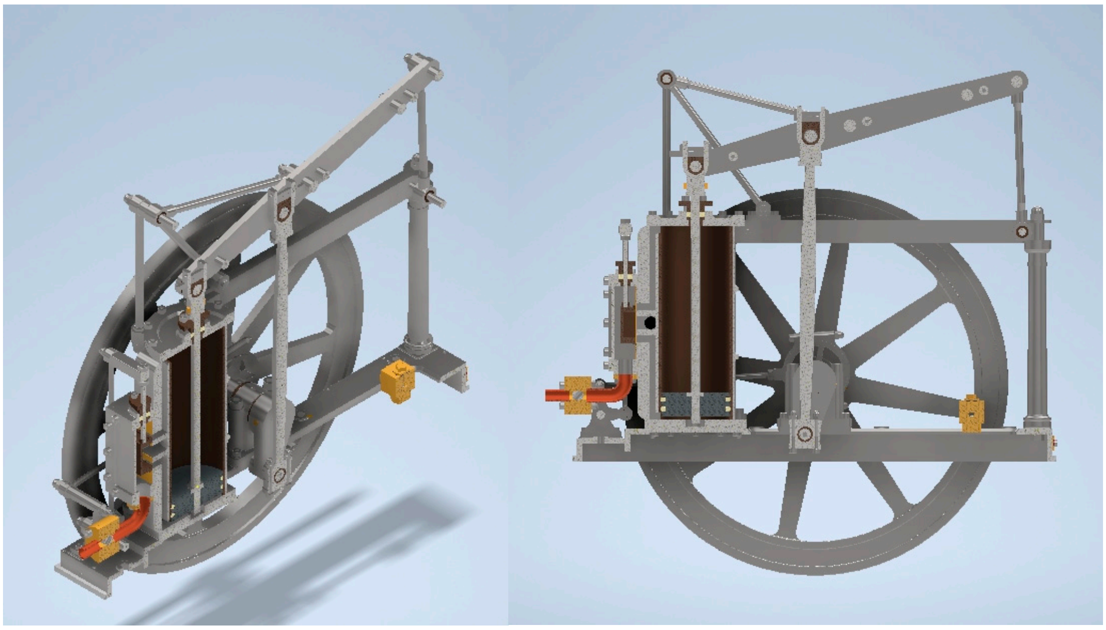

Figure 4. Sectioned views of the assembly: axonometric view (**left**) and front view (**right**).

2.2. Analysis from the Mechanical Engineering Point of View

This section explains all the stages of the process followed to carry out an analysis using the finite element method, as well as all the established working hypotheses. The stages are as follows:

- Pre-processing;
- Assignment of materials;
- Application of contacts;
- Boundary conditions;
- Discretization.

Subsequently, and once the previous stages have been carried out, a modal analysis was performed to determine the natural vibration frequencies of the machine, as well as a linear static analysis in the two critical positions of the piston plunger (lower dead center and upper dead center) which constitute the two critical positions analyzed.

2.2.1. Pre-Processing

An analysis could be carried out that included the steam engine as a whole, but due to the high number of components (more than 150) that make it up, the computational cost would be very high, and so would the simulation time. For this reason, elements that will not significantly influence the results obtained have been excluded from the analysis, given that their operating conditions will be far from critical (for safety factors regarding the unity). These excluded components are:

- Pump: The function of this element is to compress the fluid (water vapor) before it enters the boiler. Since the variation in the pressure of the fluid will depend on the speed of rotation of the machine, this pump has been suppressed and only the stresses in the pump piston will be analyzed.
- Intake and regulation system: The speed regulator has a dynamic functionality as it will rotate at a speed proportional to that of the crankshaft and this will create more or less centrifugal force, so it would make more sense to analyze this component within a dynamic analysis. Similarly, the entry of steam through the intake housing, in which the flow control valve is located, will be eliminated from the analysis to simplify the model, since this could be analyzed separately simply by applying a pressure load on the contours of the elements through which the fluid passes.

- Union elements: Many fixing elements have been suppressed and replaced by contact relationships of the 'bonded' type, that is, by welded unions. This type of contact establishes that the nodes of the meshes of the elements whose surfaces are in contact will not have relative movement between them on these surfaces. Given that in most cases, welded joints have a higher resistance than bolted joints, this simplification will make sense. This can be achieved as long as the von Mises stresses (which will be used as the failure criterion by comparing them with the yield strength) in the joint areas are far from failure (safety factor greater than unity). This will ensure that the tension in these zones continues to work in safe conditions and there is no plasticization in the joints. That is to say, if the welded joint resulted in a stress lower than the yield strength, the stress that would occur in the case of a bolted joint would be slightly higher. In Figure 5, the simplified model is shown.

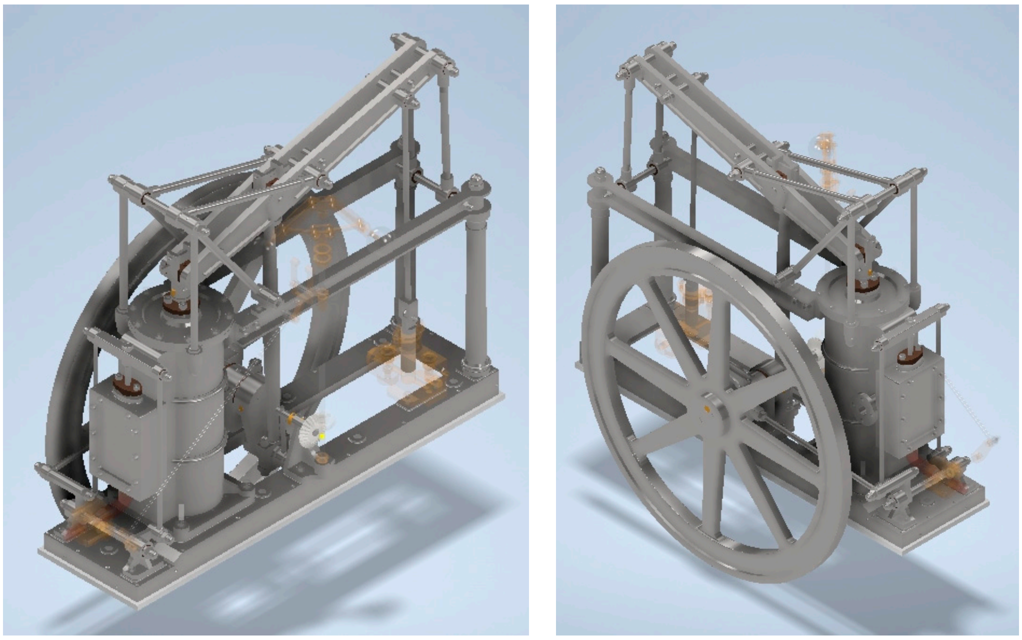

Figure 5. Simplified model of the assembly: front view (**left**) and rear view (**right**).

2.2.2. Assignment of Materials

The assignment of materials to the parts during the 3D CAD modeling with their corresponding mechanical and thermal properties is essential, since it will directly influence the behavior of the element in the analysis to be performed.

If during the modeling of each of these, the material is assigned to them, when opening the Autodesk Inventor Nastran environment, in the operations tree in the 'Model' tab, the idealizations of the materials can be found. For the invention under study, the assigned materials are the same as those assigned to each piece by the author of the plans: steel, carbon steel, stainless steel, cast iron, brass, cast bronze, rubber and nylon. Table 1 presents the values of the properties of the materials used in the analysis.

Table 1. Properties of each material used in the analysis.

Material	Young's Modulus (MPa)	Poisson Coefficient	Density (Kg/m^3)	Yield Strength (MPa)
Carbon Steel	200,000	0.290	7850	350.00
Stainless Steel	193,000	0.300	8000	250.00
Cast Iron	120,500	0.300	7150	758.00
Brass	109,600	0.331	8470	103.40
Cast bronze	109,600	0.335	8870	128.00
Nylon	2930	0.350	1130	82.75

2.2.3. Application of Contacts

For a correct simulation by the finite element method, it must be established what types of contacts there are between the elements that make up the assembly. Autodesk Inventor Nastran allows existing contacts to be established automatically, which is very advantageous since for assemblies with a high number of components, the number of contacts to be established manually would be very high and would take too much time. Therefore, it was decided to automate this process. The existing contacts in the machine are briefly explained below:

- 'Separation' type: This is the most common contact between two elements. In this type of contact, the relative movement between the nodes of the elements in contact is allowed, but with a coefficient of friction (which will be that of the materials). Apart from that, the coefficient of friction depends on other parameters, such as the surface finish of the surfaces in contact, temperature, surface roughness, etc. To simplify, a coefficient of 0.25 was applied between surfaces without lubrication, and a coefficient of 0.1 between surfaces with lubrication, for example, in bearings.
- 'Bonded' type: In this type of contact, relative movement between nodes is not allowed; that is, it behaves as if the elements in contact were welded.
- 'Symmetric/Unsymmetric contact' penetration type: In the case of symmetric penetration, the nodes of a mesh cannot penetrate the nodes of the adjacent mesh, and in the case of the asymmetric type, the penetration of nodes in adjacent meshes in contact is allowed.

One drawback that appears with the generation of contacts automatically is that the software will only make them of one type. Therefore, the behavior of the resulting mathematical model would not correspond to the behavior of the real model, since there are different types of contact in the assembly.

To solve this problem, there are two possible solutions: the first one is to establish the contacts manually, a long and tedious process since there is a large number of components, and the second option is to establish the contacts automatically and modify those that require it. The latter is the option chosen in this investigation, automatically establishing 'bonded'-type contacts, and modifying them to a 'separation'-type contact for those that require it. In this way, a response of the mathematical model that corresponds to that of the real model is achieved.

Figure 6 shows an example of the modification of a bonded contact to a separation contact (a pop-up is displayed to change the contact type between a bearing and the head of a beam).

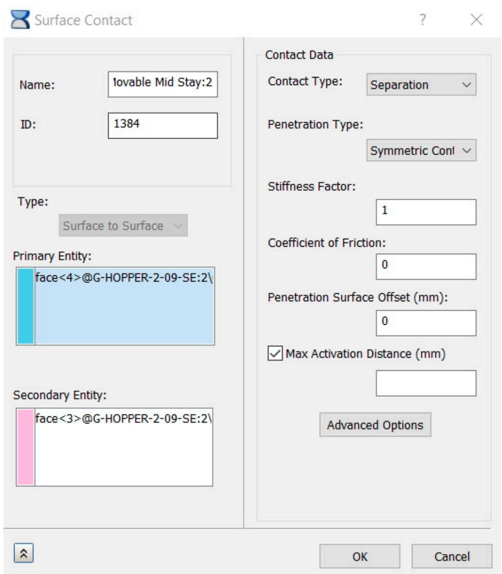

Figure 6. Pop-up to modify the contact type.

2.2.4. Boundary Conditions

In order to carry out a coherent analysis, the boundary conditions that will restrict certain degrees of freedom of the components of the invention must be established, in order to obtain results that are as close as possible to those obtained in real operating conditions.

First, all the lower faces of the bedplate were fixed without any movement (all freedom degrees are restricted) (Figure 7); that is to say, they are prevented from any displacement and rotation. This boundary condition would be equivalent to fixing the bedplate of the steam engine to the ground, or to the chassis of the train or ship where the steam engine was located.

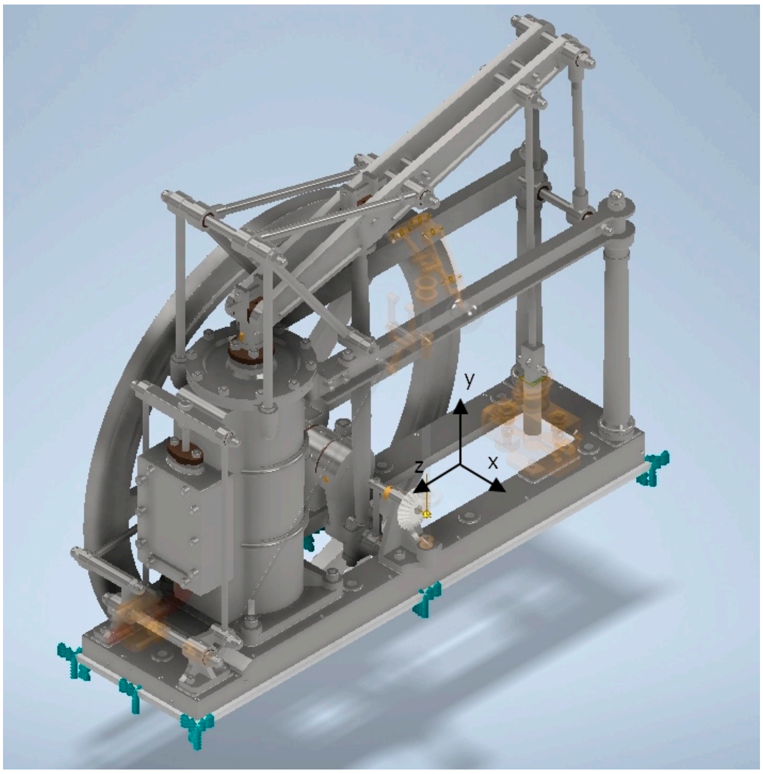

Figure 7. Bedplate boundary conditions.

Secondly, as the pump has been eliminated in the simplified model for analysis, the movement of its piston must be restricted (Figure 8), since it would have an alternative movement in the vertical direction with respect to the pump. Therefore, all displacements are restricted except for the displacement, whose direction coincides with the longitudinal axle of the pump piston. In turn, since two cap nuts that hold the pin that joins the pump piston to the rod have been eliminated in order to simplify the analysis, horizontal displacement (direction of the axis of revolution of the pin) is prevented in order to obtain an operation similar to that which would be obtained in the case of carrying out the analysis with these cap nuts. In Figure 9, the restricted degrees of freedom for the piston pump (those with a tick) are shown.

Finally, since a linear static analysis is going to be carried out simulating the two most critical positions (piston plunger at lower dead center and at upper dead center), the flywheel is fixed (all freedom degrees are restricted) (Figure 10). In this way, the invention will be blocked and the output variables (stress, displacement and safety factor) will be analyzed in both critical positions. In Section 2.2.6, these critical positions are explained in detail, as well as the reason for choosing them among all the possible ones.

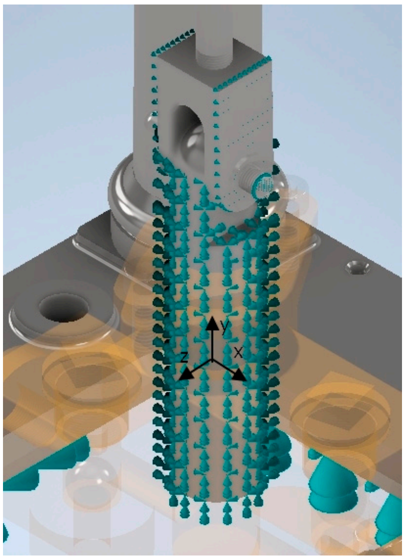

Figure 8. Pump piston boundary conditions.

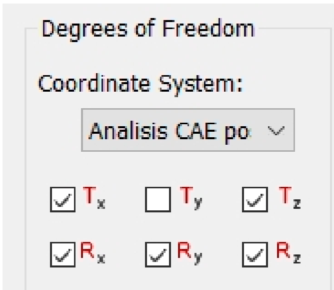

Figure 9. Restricted degrees of freedom for the piston pump.

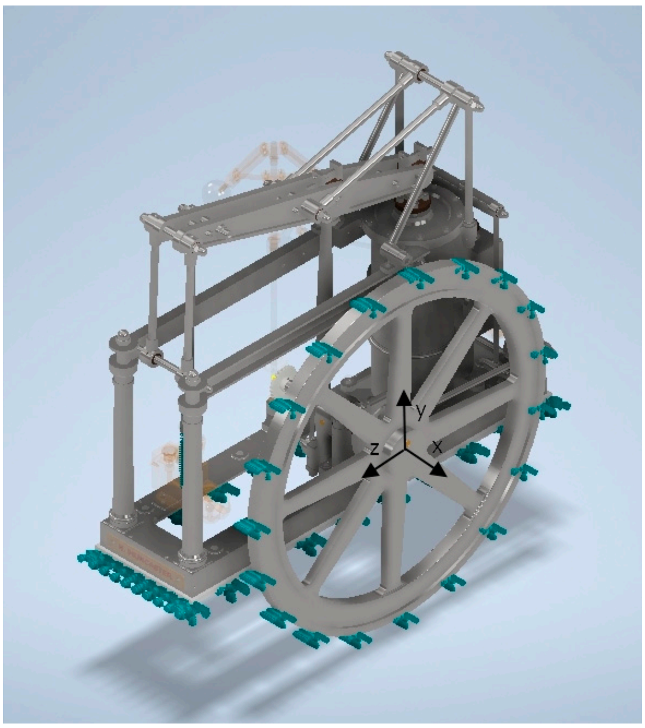

Figure 10. Flywheel boundary conditions.

2.2.5. Discretization

To finish with the steps prior to the analysis, the continuous medium must be discretized. Discretization consists of dividing the continuum medium into numerous elements defined by nodes. In this way, the analysis variables will be calculated in the nodes of the elements, and the values will be interpolated in them in order to obtain the value inside the element. Depending on the number of nodes that the element has, the interpolation order will vary.

This discretization is necessary in order to be able to carry out the analysis, since the differential equations that govern the behavior of the continuous medium cannot be solved. Therefore, the finite element method is used to obtain an approximate solution to these equations. The error committed between the analysis by the finite element method, and the real case for solving the differential equations, will depend on the grid size.

After this brief description of the finite element method and the need to apply it in order to solve the problem, the discretization for the case study is presented (Figure 11).

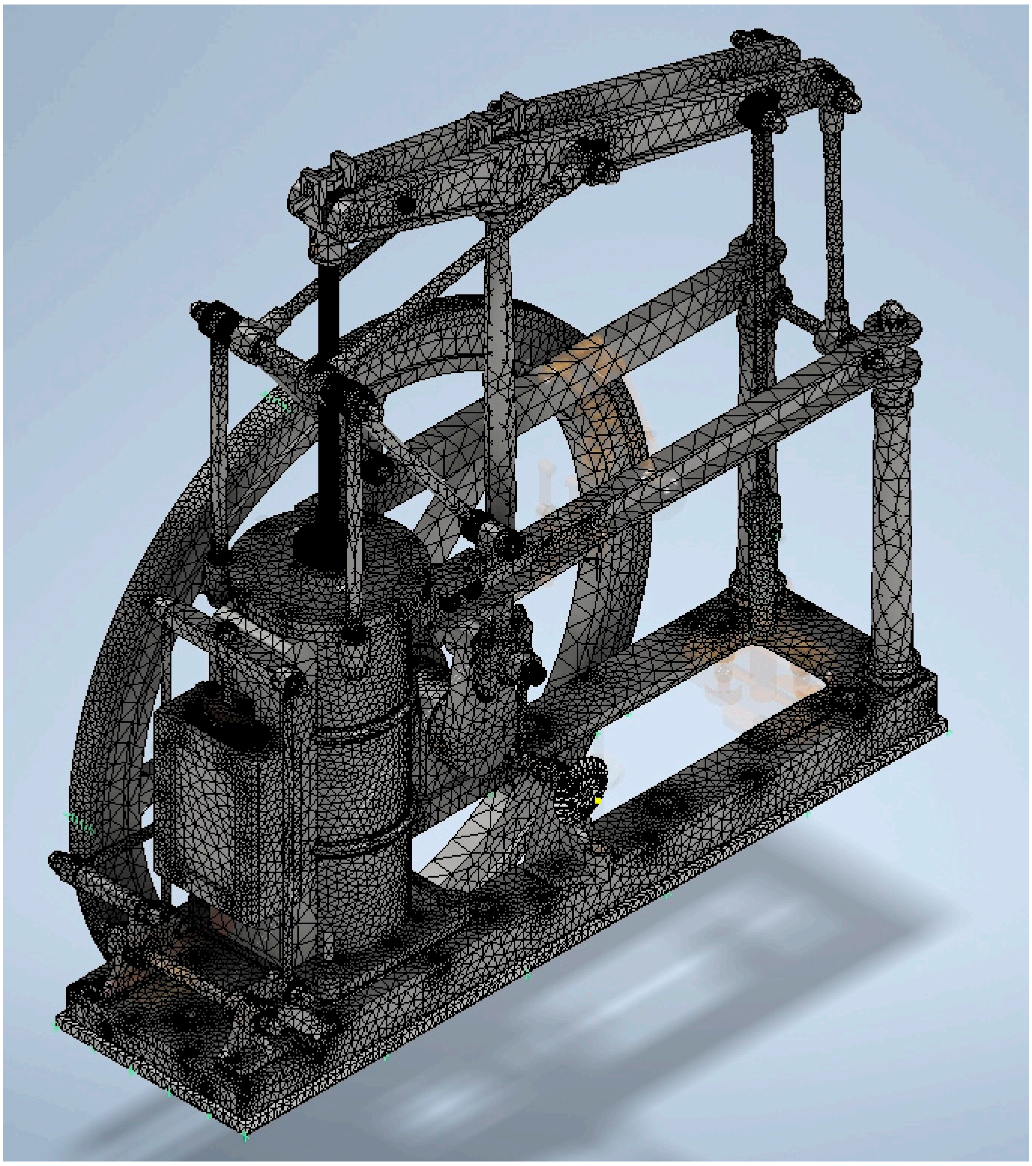

Figure 11. Axonometric view of the discretization of the assembly.

In the present investigation, quadratic interpolation order elements were used, that is, parabolic-type elements (tetrahedra) (Figure 12), to obtain more precise results inside the finite element. The software automatically generates a smaller mesh in smaller parts so that the grid fits better to the geometry of the part and the results are more accurate. Thus, the maximum element size (0.029 m) and the maximum element growth ratio (1.1) have been defined. This configuration allows greater control over the mesh of the parts with contacts, meaning less distortion of the elements. In addition, Autodesk Inventor Nastran allows a more advanced configuration of the finite elements, being able to modify the maximum and minimum angles of the triangle of the tetrahedron. Moreover, the growth rate of the element can be modified in contact zones between different solids, as well as in edges or vertices where a smaller element is required for a better adaptation to the geometry of the solid. In this way, a higher-quality mesh is achieved, and, as they are tetrahedrons, a better adaptation to the geometry of each solid. In this investigation, the analysis used a mesh size of 1,132,720 elements and 1,696,754 nodes.

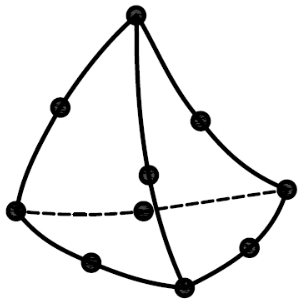

Figure 12. Finite element used. Tetrahedron of quadratic interpolation.

2.2.6. Critical Positions

The piston plunger positions that give rise to the greatest von Mises stress and the largest magnitude displacements should be analyzed, since although many positions could be analyzed, the ones of greatest interest are those that will subject the machine to the conditions of most critical operation.

For the case study, two critical positions are presented (Figure 13), corresponding to the position of the piston plunger at the lower dead center and the upper dead center after closing the steam intake by the slide valve in order to later expand inside the cylinder chamber and produce work. In addition, since it is a double-acting steam engine, both situations must be taken into account. In these positions, the maximum pressure is exerted on one of the faces of the piston and atmospheric pressure on the opposite face, since when the steam is renewed in one of the chambers, the discharge or exhaust occurs in the other, and at that instant, the pressure on the face of the piston and cylinder chamber is atmospheric pressure. Once the piston reaches one of these two critical positions, the pressure inside one of the chambers is at its maximum, and the pressure will produce greater stresses and deformations.

Moreover, since the flywheel is blocked, it will be possible to simulate in this way the placing of the machine in operation and observe how the force is transmitted from the piston to the rest of the elements of the steam engine. This blocking situation can be assimilated to a very common test in reciprocating and rotary internal combustion engines, since the torque present on the engine shaft is measured by braking the flywheel. Figure 13 shows the invention in both critical positions, clearly observing the position of the elements, particularly that of the balance beam, since it is the most innovative element of the invention for the time in which it was developed.

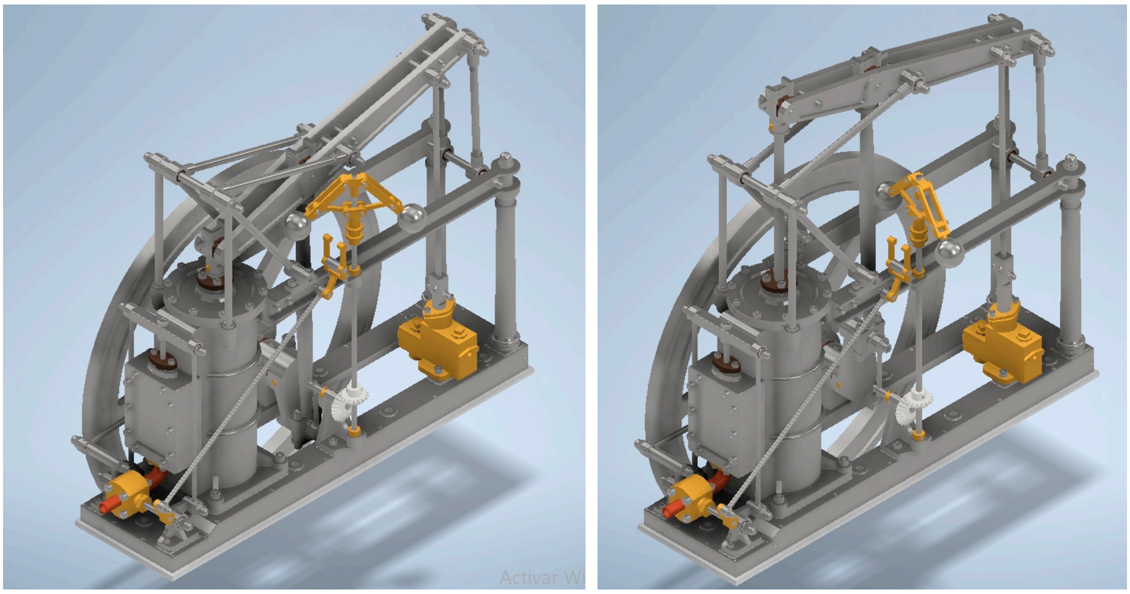

Figure 13. Axonometric views of the critical positions: lower dead center (**left**) and upper dead center (**right**).

2.2.7. Modal Analysis

Every mechanical system has natural frequencies of vibration and has as many modes of vibration (natural frequencies) as degrees of freedom. Each vibration mode is characterized by a frequency (Hz) and a vibration mode (mode number). This is the consequence of subjecting the system to an imbalance caused by the application of an external force. If this external force takes the solid to a deformed position (within the linear elastic regime, without presenting permanent plastic deformations) and suddenly disappears, the solid will return to its original equilibrium position, but it will arrive with certain kinetic energy (since when it stops the force, the potential energy stored by the material is transformed into kinetic energy) that will cause deformation to occur in the opposite direction to that created by the external force, returning to seek the equilibrium position, and thus producing vibration. When the system vibrates, it will do so at a series of frequencies, these being the natural frequencies.

Therefore, since a linear static analysis is to be carried out later, it does not make sense to execute it if any of the vibration modes of the system (steam engine) corresponds to a frequency of 0 Hz, since it would behave like a mechanism. In this way, for both critical positions of the assembly, the first 10 natural frequencies were obtained, and it was verified that all of them are greater than 0.

2.2.8. Linear Static Analysis

As previously mentioned, the analysis to be carried out will be linear static, after verifying that the system does not have any vibration mode corresponding to the frequency of 0 Hz. This analysis will force a convergence analysis of the mesh to ensure that the results obtained are correct and that this convergence approaches the real solution. Therefore, the objective of the convergence analysis is to observe for what value of the element size the von Mises stress does not vary to a large extent.

Determination of the Strain Envelope

The correct determination of the strain envelope is essential for a correct analysis that does not lead to erroneous results.

The plans [7] that have made it possible to obtain the 3D CAD model of the invention show its reduced dimensions. As mentioned previously, the main application of this machine was its use in small boats and trains, so its dimensions would be larger depending on the size of the means of locomotion.

Despite all this, and as a starting point, an analysis was carried out for a manometric working pressure of 0.75 MPa, since exact information on the operating conditions of the machine is not available. The steam conditions at the cylinder inlet depend on the geometry of the machine, that is, the dimensions of the plunger, the chamber, etc., as well as the application. For use in maritime vessels or trains, the pressure value could range between 1 and 8 MPa, depending on the machine, and in power plants for the generation of electrical energy, the outlet pressure of the boiler could have a value greater than 10 MPa. This pressure is produced by the steam that comes out of the boiler, being applied in the slide valve chest block, the slide valve and the corresponding piston face, depending on the position. Therefore, this manometric pressure value is used, because throughout the invention in its environment, and in the chamber opposite to the pressure application chamber, there will be an applied pressure of a value equal to atmospheric pressure. In addition, after expanding the steam inside the chamber, the exhaust valve opens and the steam escapes at a constant pressure equal to atmospheric pressure, while in the other chamber, the admission of steam will be taking place at the working pressure.

After the application of the pressure of 0.75 MPa, the behavior of the machine can be observed, and if the minimum safety factor is less than the unity, the steam engine will have exceeded the yield strength and therefore, it will fail at the first cycle static charge. In this way, several analyses must be carried out until a pressure value is determined that causes a maximum von Mises stress lower than the yield strength value, and whose safety factor is greater than the unity for the machine to work safely (values between two and four are those used when designing machines today).

In Figure 14, the application of the pressure loads for the critical position corresponding to the position of the piston plunger at the lower dead center can be seen in detail.

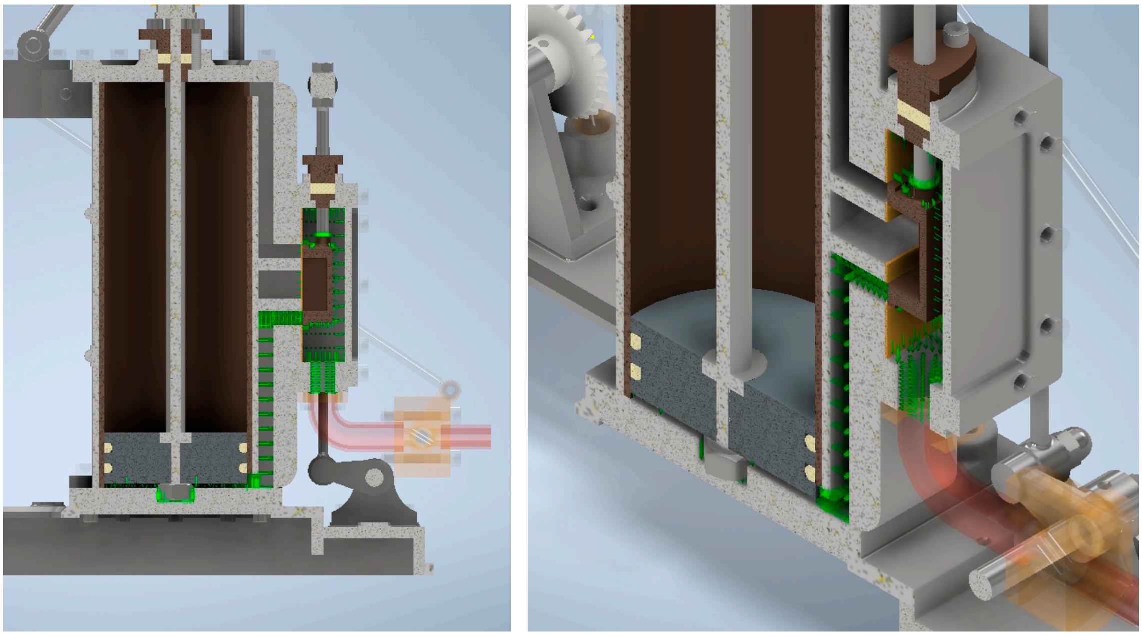

Figure 14. Pressure loads at the lower dead center position: front view (**left**) and axonometric view (**right**).

In the same way, the pressure load for the critical position corresponding to the upper dead center would be applied. In that case, the load would be applied to the opposite face of the piston with respect to the lower dead center position. In this way, it will be possible to observe two critical and opposite behaviors, given that for the lower dead center position, the piston rod will work in compression while for the upper dead center, the piston rod will work in traction. Viewed in this way, a more critical behavior can be anticipated in the upstroke of the piston, that is, for movement from the lower dead center to the upper dead center. The fact that the piston rod works in compression instead of traction produces greater criticality in the deformed state, since a compression load can give rise to eccentricity of the applied load if the piston rod deforms, producing buckling. For this reason, it is foreseen that the most critical position will be the position of the lower dead center.

Analysis Execution

After applying the pressure loads, the analysis will be carried out. Autodesk Inventor Nastran allows users to automatically perform several iterations in the simulation to determine the convergence of the mesh. Finally, a graph will be obtained for the convergence analysis as well as the response of the steam engine to the load, quantified by the values of the von Mises stress and by the displacements, as well as the safety factor defined as the quotient between the yield strength of the material and the von Mises stress at a given point.

The steam engine is an assembly with a high number of components, obtaining a very complex mesh with a high computational cost in the simulation. However, the mesh convergence analysis performed by the software itself reaches convergence in two iterations. For this reason, in order to ensure that the results offered by the software are completely reliable, it was decided to carry out a mesh convergence analysis manually, the results being those corresponding to the manual mesh convergence analysis. This analysis consists of performing a first mesh with a determined global mesh size and proceeding to the simulation. Once the results are obtained, the place where the external strains give rise to a maximum von Mises stress can be determined, noting this value together with the iteration number and the element size.

The next step is to perform a local mesh control in the area of maximum stress, reducing the size of the finite element in that area. Control can be achieved in several ways: by refining vertices, edges, surfaces or solids. For the case study, it was decided to completely refine the solid (piston rod) where the maximum stresses are produced. Once the value of the size of the element has been reduced, the meshing of the assembly is carried out again and the simulation is repeated. This process is repeated until the relative error of the von Mises stresses between iteration (i) and iteration (i-1) is less than an established percentage (in the present investigation, a value of 10% was adopted).

3. Results and Discussion

This section presents the results obtained for the modal analysis and linear static analysis in each of the two critical positions studied. It should be noted that the figures presenting the analysis results are screenshots taken from the software (Autodesk Inventor Nastran), which uses the comma as the decimal separator instead of the dot.

3.1. Critical Position: Lower Dead Center

3.1.1. Modal Analysis

After applying the corresponding boundary conditions, the simulation is performed in Autodesk Inventor Nastran. Figure 15 shows a graph in which the abscissa axis corresponds to the mode number of the vibration and the ordinate axis to the natural frequency (Hz) corresponding to this mode number.

The graph shows how vibration mode 1 corresponds to a frequency value greater than 200 Hz, this being the lowest of its natural vibration frequencies. Therefore, a static analysis can be performed since it will not behave as a mechanism under the simulation conditions at the critical position corresponding to the position of the piston plunger at the lower dead center.

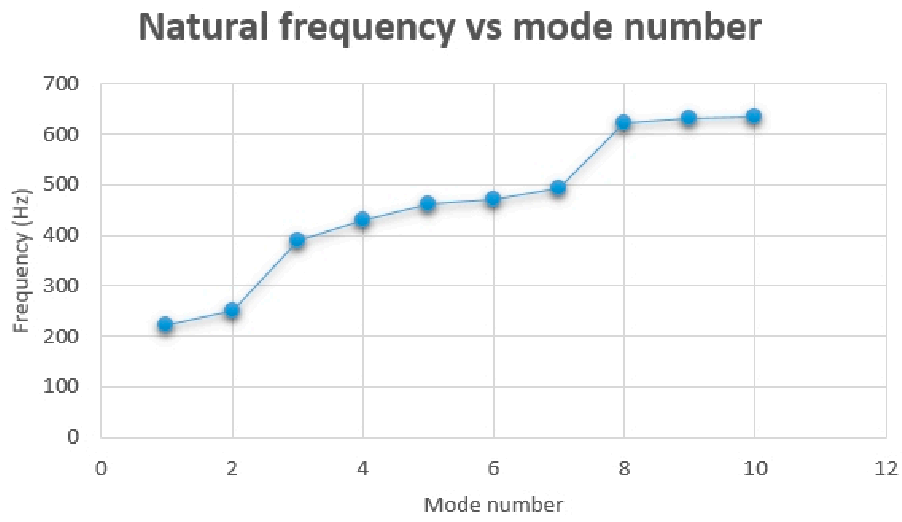

Figure 15. Natural frequency vs. mode number of the vibration.

Thus, the first 10 natural frequencies of vibration for the steam engine at this critical position are 221.17 Hz, 249.73 Hz, 390.74 Hz, 431.69 Hz, 460.54 Hz, 470.16 Hz, 493.69 Hz, 623.09 Hz, 632.22 Hz and 636.54 Hz. A system has as many natural frequencies as degrees of freedom, but it does not make sense to obtain all the natural frequencies since only those with the lowest value are of interest in order to rule out the possibility that the invention behaves like a mechanism (this is for a natural frequency of vibration of 0 Hz) and to carry out static analysis.

3.1.2. Linear Static Analysis

Below, the results are presented for the critical position corresponding to the lower dead center, after closing the steam intake to the cylinder for its subsequent expansion inside the chamber.

As previously explained, first, a linear static analysis was carried out under a pressure of 0.75 MPa, producing a maximum von Mises stress of 1089 MPa at the top of the piston rod (Figure 16).

This value of the von Mises stress results in a safety factor less than the unity (0.51). Therefore, it can be stated that the machine would fail if the steam pressure at the intake was 0.75 MPa. This makes it necessary to carry out another analysis to obtain a lower value of the von Mises stress, particularly 0.15 MPa, and to analyze the results to determine whether this value of steam pressure is adequate for the correct operation of the machine.

The analysis carried out above not only indicates that the machine fails, but also offers information on the place where the maximum von Mises stress is located, particularly at the top of the piston rod. This will make it possible to perform a mesh refinement in that area and to study the convergence of the mesh, comparing the element size with the value obtained from the von Mises stress.

After performing the analysis with different mesh sizes in the piston rod, the convergence analysis graph of the mesh is obtained (Figure 17), as well as the table with the size of the element, the von stress Mises, the relative error (%) and the iteration number (Table 2).

From Table 2, it can be seen that the relative error obtained for an element size of 0.4 mm is 7.35%. The computational limitations for the development of the analysis and the complexity of the assembly do not allow further refinement of the mesh in the piston rod, which is the most critical element. Despite this, an error slightly higher than 7% offers good results, and since the purpose of the analysis is only to obtain information about the design of the invention, this relative error can be accepted.

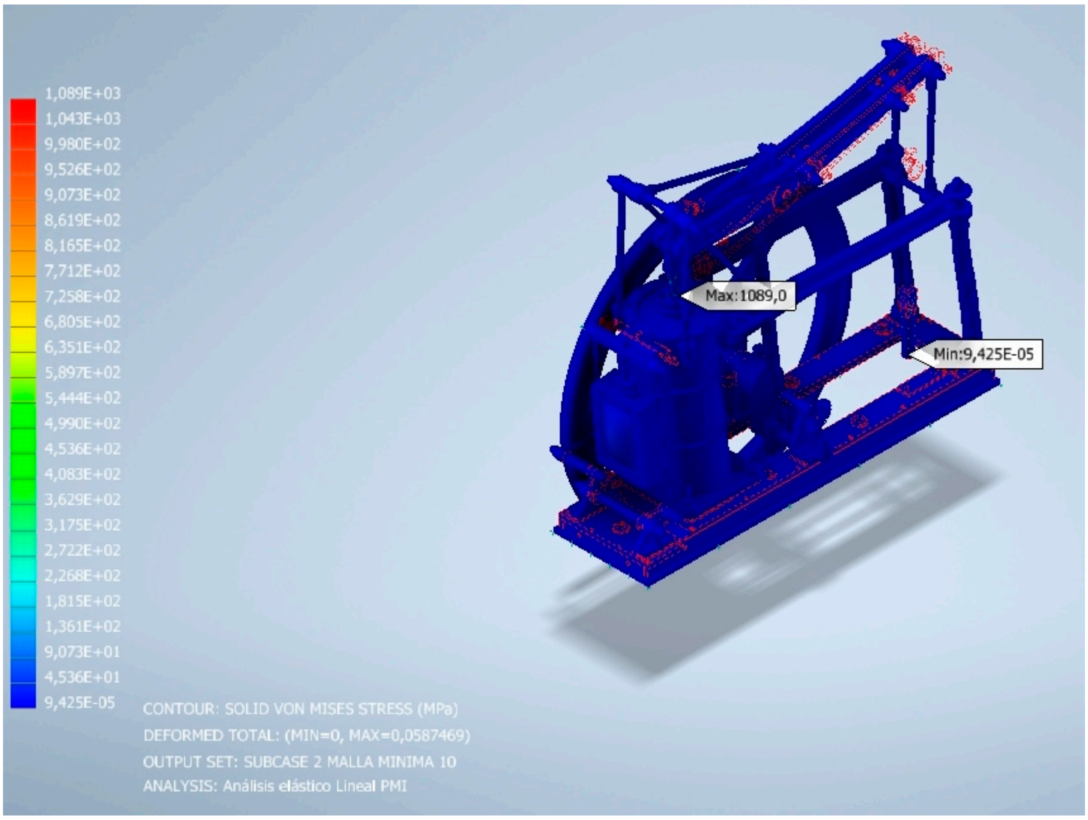

Figure 16. Von Mises stress distribution for a pressure of 0.75 MPa.

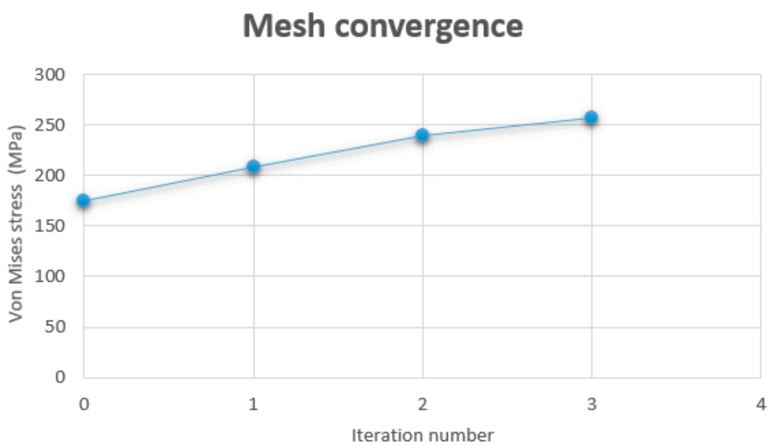

Figure 17. Mesh convergence graph.

Table 2. Mesh convergence analysis.

Element Size (mm)	Von Mises Stress (MPa)	Relative Error (%)	Iteration
1.5	175.5		0
1	208.1	18.58	1
0.5	239.4	15.04	2
0.4	257	7.35	3

Below are shown the von Mises stress distribution (Figure 18) and the exact location (piston rod) of its highest value (257 MPa) (Figure 19). In addition, it should be noted that the von Mises stress, displacements and safety factor distributions were obtained on the deformed position of the invention multiplied by a factor of value 10, in order to clearly observe the shape that the assembly adopts in the deformed position, since for a value factor of the unity, the deformed position could hardly be seen due to the very small value of the displacements obtained.

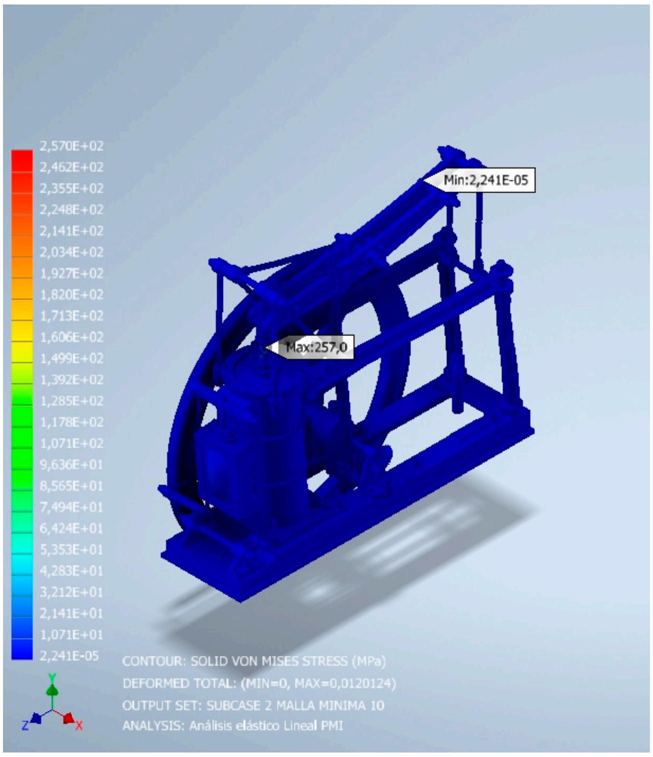

Figure 18. Von Mises stress distribution.

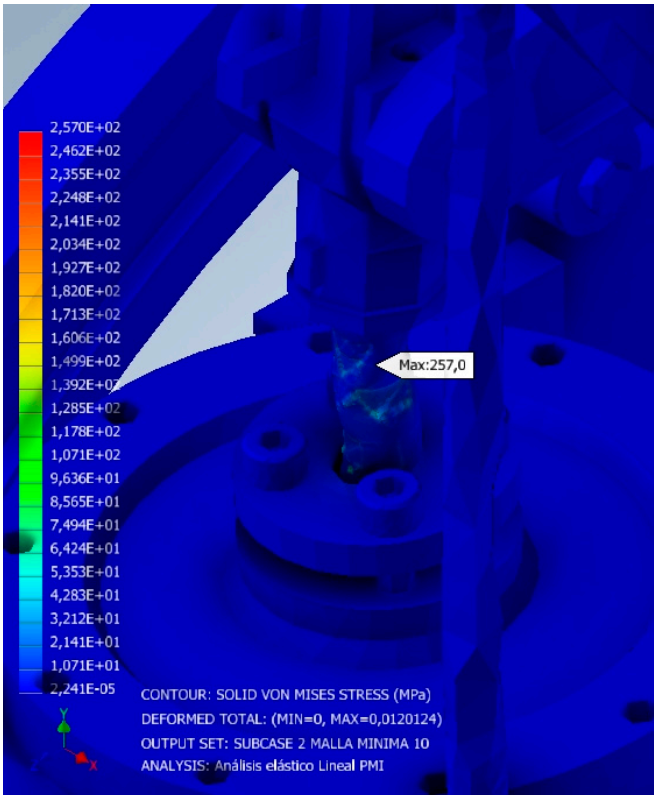

Figure 19. Location of the highest von Mises stress.

On the other hand, Figure 20 represents the distribution of displacements, in which it can be seen that these are negligible.

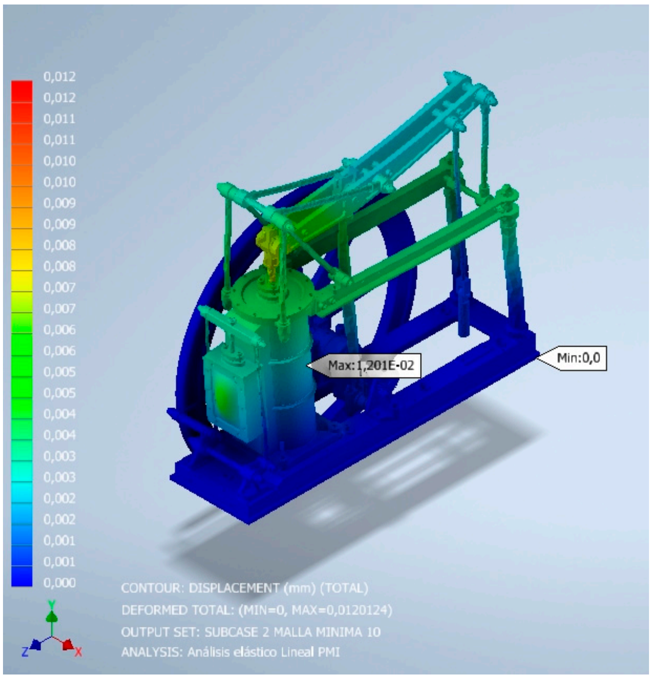

Figure 20. Displacement distribution.

Figure 21 shows the safety factor, defined as the result of dividing the yield strength of the material by the value of the von Mises stress at a specific point. In this figure, it can be seen that the smallest value of the safety factor is 2.307, located at the piston rod.

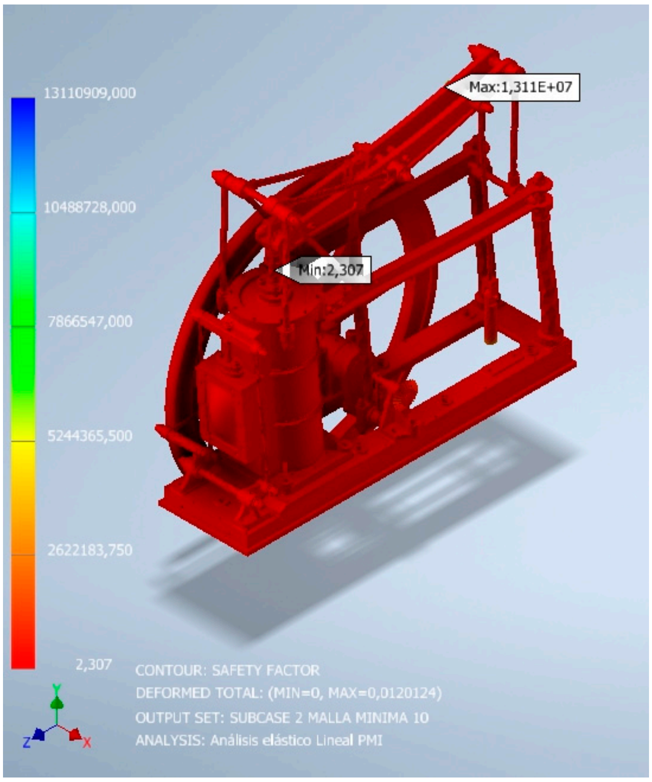

Figure 21. Location of the lowest value of the safety factor.

3.2. Critical Position: Upper Dead Center

3.2.1. Modal Analysis

After applying the corresponding boundary conditions, the simulation was performed in Autodesk Inventor Nastran. Figure 22 shows a graph in which the abscissa axis corresponds to the mode number of the vibration, and the ordinate axis to the natural frequency (Hz) corresponding to this mode number.

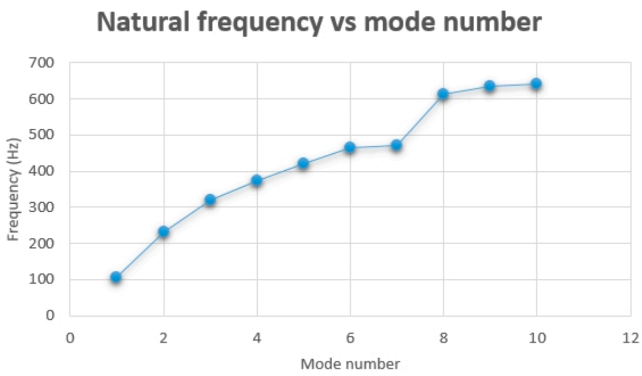

Figure 22. Natural frequency vs. mode number of the vibration.

The values of the first 10 natural frequencies are as follows: 105.34 Hz, 232.40 Hz, 319.77 Hz, 375.03 Hz, 422.13 Hz, 464.58 Hz, 472.74 Hz, 613.48 Hz, 634.45 Hz and 640.17 Hz.

As in the case of the critical position corresponding to the lower dead center, since the natural frequency associated with the first mode of vibration is greater than 0 Hz, linear static analysis can be performed at the critical position of the upper dead center, since this would not behave like a mechanism.

3.2.2. Linear Static Analysis

Next, as for the lower dead center critical position, the value obtained for each of the variables of interest is shown, that is, the von Mises stress, displacement and safety factor, as well as a graph of the convergence analysis of the mesh (Figure 23) and the table with the element size, the von Mises stress, the relative error (%) and the iteration number (Table 3). All these values were obtained for the same working pressure adopted for the lower dead center of value 0.15MPa, it being necessary to verify that, for this critical position, and at said working pressure, the safety factor is greater than the unity, thus ensuring the operation of the steam engine under safe conditions and that there is no failure under the static load of the first cycle.

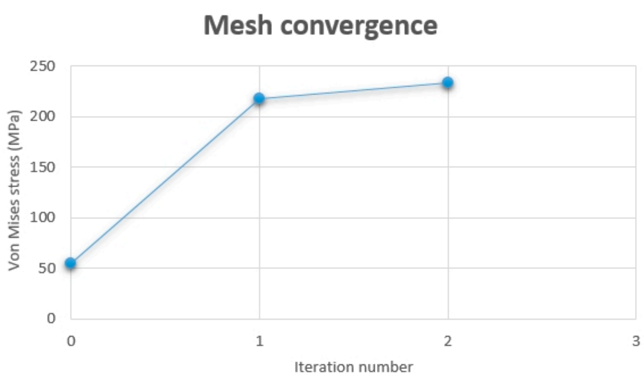

Figure 23. Mesh convergence graph.

These results are the ones obtained for the indicated mesh element sizes, refining the piston rod, since the maximum von Mises stress in the piston rod is obtained in the first iteration (iteration 0). Thus, in the following iterations, the analysis is executed by applying a local mesh control on that piston rod, thereby reducing the size of the finite element until the solution converges (relative error less than 10%).

Table 3. Mesh convergence analysis.

Element Size (mm)	Von Mises Stress (MPa)	Relative Error (%)	Iteration
2	54.9		0
1.5	217.8	296.64	1
0.75	233.4	7.16	2

In the same way as in the lower dead center critical position, and given the computational limitations and the complexity of the machine, the mesh cannot be further refined.

The von Mises stress distribution is shown below (Figure 24), as well as an enlarged view of the location (piston rod) of the highest value obtained (233.4 MPa) (Figure 25).

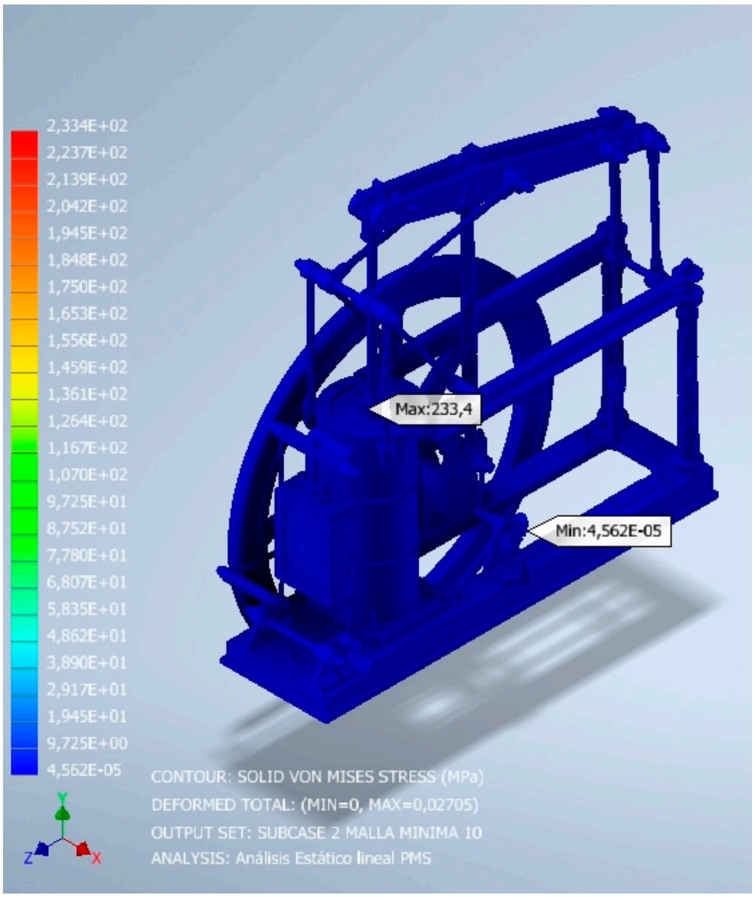

Figure 24. Von Mises stress distribution.

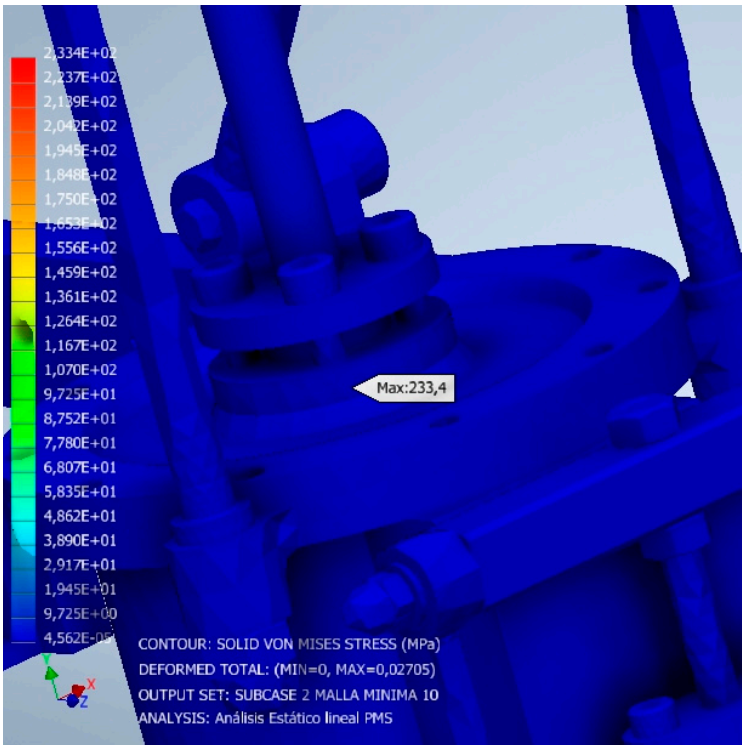

Figure 25. Location of the highest von Mises stress.

Figure 26 represents the distribution of displacements, in which it can be seen that they are negligible.

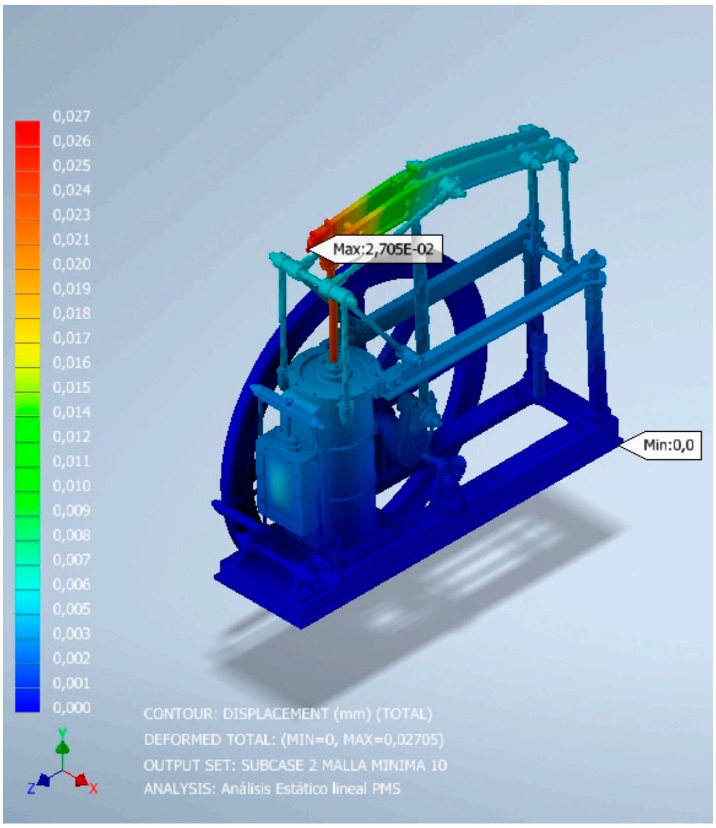

Figure 26. Displacement distribution.

Finally, Figure 27 shows the distribution of the safety coefficient for this critical position and the location of the lowest value of this coefficient (1.445), located at the piston rod.

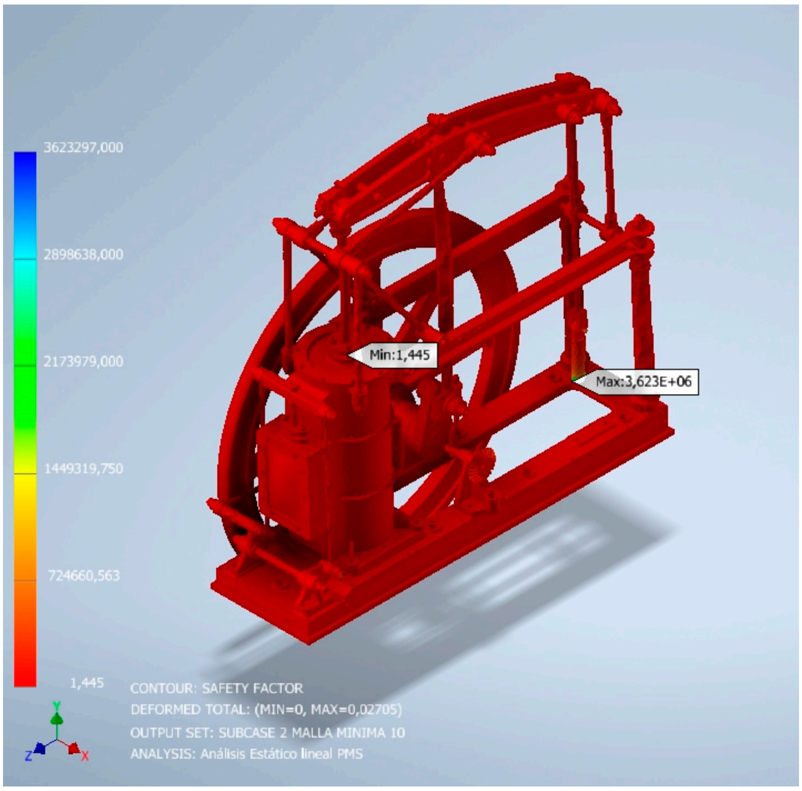

Figure 27. Location of the lowest value of the safety factor.

3.3. Discussion of the Results

According to the results, the highest von Mises stress was obtained in the critical position of the lower dead center. In this position, there is a compression load that can cause buckling of the piston rod. Therefore, in future research, this rod could be analyzed in order to determine whether the rod complies under the buckling failure criterion.

Regarding the displacements, and as previously indicated, an increase factor of 10 was applied in order to more clearly observe the deformed position of the steam engine in both critical positions (lower and upper dead center), so that the representation is not the real one. In both analyses, practically negligible displacements were obtained. This favors the proper functioning of the steam engine under this pressure load, since the hypothesis of small deformations can be applied and the strains in the undeformed position can be calculated (that is, using the Eulerian formulation method for meshing, which reduces the computational cost). In addition, since there are no large deformations, the relative movement between the elements will give rise to the least possible friction, since, for example, if there were large deflections in the piston rod, there would be greater friction contact in the bushing and piston seal itself, and mechanical energy would be lost.

Finally, as desired, the safety factor is greater than the unity, so it can be stated that the machine does not fail under the first cycle static load at a working pressure of 0.15 MPa. However, even though the maximum von Mises stress at the upper dead center is less than that obtained at the lower dead center, the safety factor is also less. This is due to the fact that higher stress is produced in a secondary element than in the lower dead center analysis, and its mechanical characteristics (Young's modulus and yield strength) are lower than those of the piston rod.

Therefore, with the present research, it has been possible to determine the maximum admissible steam pressure in the admission (working pressure) for this machine, corresponding to 0.15 MPa. This value can be used to determine the working pressure in other similar machines, relating the parameters of both models through dimensional analysis.

4. Conclusions

In this paper, the design of the single-cylinder steam engine of the Grasshopper beam by Henry Muncaster according to material resistance criteria was analyzed. In the absence of detailed information on the operating data of the invention, this double-acting steam engine was studied with computer-aided engineering techniques, specifically through linear static analysis, in the two critical positions: when the piston rod is at the lower dead center and at the upper dead center. This was possible thanks to the Autodesk Inventor Nastran software.

The objective of this research was to study from the design point of view what would be the maximum admissible steam pressure in the admission (working pressure) so that the invention would not fail, according to material resistance criteria, thus analyzing von Mises stresses, displacements and safety factors.

Thus, after manual refining, a mesh convergence analysis was performed, obtaining a relative error of 7.35% and an element size of 0.4 mm for the position of the piston plunger at the lower dead center, and a relative error of 7.16% and an element size of 0.75 mm for the upper dead center position. The iterative process then stopped at the fourth iteration for the lower dead center position, and at the third iteration for the upper dead center position, taking into account that the first iteration was carried out to estimate the zone of greatest criticality of the invention in both positions.

On the other hand, the highest von Mises stress for the working pressure (0.15 MPa) obtained a value of 257 and 233.4 MPa in both critical positions (lower and upper dead center, respectively), being located on the piston rod. Furthermore, the minimum safety factors were greater than the unity (2.307 and 1.445 in lower and upper dead center, respectively), guaranteeing that the invention did not fail.

In addition, and as possible future research, a dimensional analysis could be carried out from the determination of the working pressure (0.15 MPa) that relates this pressure to the relevant dimensions of the machine, such as the diameter and stroke of the piston plunger, in order to be able to extrapolate results to a similar invention (same geometric characteristics but different dimensions). This would allow the number of analyses to be reduced, since carrying out tests for a single machine would allow values to be extrapolated to other similar machines. Another advantage of applying the dimensional analysis technique to this simulation is that it not only determines the maximum operating pressure in a similar machine, but also that an inverse study can be carried out if it is required for a certain function, such as calculating the specific value of torque on the flywheel of a train that circulates at a certain speed. In this way, and based on these data, the working pressure that produces the torque is determined, analyzing the thermodynamic cycle and applying the most appropriate and effective mechanical and thermal performance and then determining the geometry necessary to produce this torque and/or effective power.

Author Contributions: Conceptualization, J.I.R.-S.; methodology, J.I.R.-S. and J.F.G.-A.; investigation, J.I.R.-S. and J.F.G.-A.; formal analysis, J.I.R.-S. and J.F.G.-A.; visualization, J.I.R.-S. and J.F.G.-A.; supervision, J.I.R.-S.; writing—original draft preparation, J.I.R.-S. and J.F.G.-A.; writing— review and editing, J.I.R.-S. and J.F.G.-A. All authors have read and agreed to the published version of the manuscript.

Funding: The research presented in this paper was possible thanks to a collaboration grant with the Department of Engineering Graphics, Design and Projects of the University of Jaen obtained in the 2022 call from the Ministry of Education and Vocational Training of the Government of Spain.

Data Availability Statement: Not applicable.

Acknowledgments: We would like to thank the anonymous reviewers of this paper for their constructive suggestions and comments.

Conflicts of Interest: The authors declare no conflict of interest.

References

1. Inkster, I. (Ed.) *History of Technology*; Bloomsbury Academic: London, UK, 2004; Volume 25.
2. Jenkins, R. *Links in the History of Engineering and Technology from Tudor Times*; The Newcomen Society at the Cambridge University Press: Cambridge, UK, 1971.
3. Russell, B. *James Watt: Making the World Anew*; Reaktion Books: London, UK, 2014.
4. Who Was Henry Muncaster? Available online: https://modelengineeringwebsite.com/Henry_Muncaster.html (accessed on 29 June 2023).
5. Muncaster, H. *Model Stationary Engines—Their Design and Construction*; TEE Publishing Ltd.: Oxford, UK, 1912.
6. Grasshopper Beam Engine. Available online: https://en.wikipedia.org/wiki/Grasshopper_beam_engine (accessed on 29 June 2023).
7. Single Cylinder Grasshopper Beam Engine. Available online: https://modelengineeringwebsite.com/Muncaster_grasshopper.html (accessed on 29 June 2023).
8. Rojas-Sola, J.I.; Gutiérrez-Antúnez, J.F. Geometric modeling and digital restitution of a single cylinder steam engine of the Grasshopper beam by Henry Muncaster. In *Advances in Engineering Design IV*, 1st ed.; Manchado del Val, C., Suffo Pino, M., Miralbés Buil, R., Moreno Sánchez, D., Moreno Nieto, F.D., Eds.; Springer: Cham, Switzerland, 2024; (*accepted for publication*).
9. Crowley, T.E. *The Beam Engine: A Massive Chapter in the History of the Steam*, 1st ed.; Senecio Publishing: Oxford, UK, 1982; pp. 64–65.
10. Semmens, P.W.B.; Goldfinch, A.J. *How Steam Locomotives Really Work*; Oxford University Press: Oxford, UK, 2003; p. 97.
11. Liu, Y.; Huang, M.; An, Q.; Bai, L.; Shang, D.Y. Dynamic characteristic analysis and structural optimization design of the large mining headrame. *Machines* **2022**, *10*, 510. [CrossRef]
12. Stavroulakis, G.E.; Charalambidi, B.G.; Koutsianitis, P. Review of computational mechanics, optimization, and machine learning tools for digital twins applied to infrastructures. *Appl. Sci.* **2022**, *12*, 11997. [CrossRef]
13. Jumper, L.; Shih, R.H. *Parametric Modeling with Autodesk Inventor 2023*; SDC Publications: Mission, KS, USA, 2022.
14. Autodesk Inventor Nastran 2023. About Tutorials. Available online: https://help.autodesk.com/view/NINCAD/2023/ENU/?guid=GUID-DB7160BE-0C72-47B9-B5EF-FC4925B455CE (accessed on 11 June 2023).